PHYSICAL REVIEW D **89,** 054036 (2014)

NNLO low-energy constants from flavor-breaking chiral sum rules based on hadronic τ-decay data

Maarten Golterman[*]

Department of Physics and Astronomy, San Francisco State University, San Francisco, California 94132, USA

Kim Maltman[†,‡]

Department of Mathematics and Statistics, York University, 4700 Keele Street, Toronto, Ontario M3J 1P3 Canada

Santiago Peris[§]

Department of Physics, Universitat Autònoma de Barcelona, E-08193 Bellaterra, Barcelona, Spain

(Received 11 February 2014; published 28 March 2014)

Using spectral data from nonstrange and strange hadronic τ decays, flavor-breaking chiral sum rules involving the flavor *ud* and *us* current-current two-point functions are constructed and used to determine the $SU(3)$ next-to-next-to-leading order (NNLO) low-energy constant combinations C^r_{61}, $C^r_{12}+C^r_{61}+C^r_{80}$ and $C^r_{12}-C^r_{61}+C^r_{80}$. The first of these determinations updates the results of an earlier analysis by Dürr and Kambor, while the latter two are new. The error on $C^r_{12}+C^r_{61}+C^r_{80}$ is particularly small. Comparisons are made to model estimates for these quantities. The role of the third combination in significantly improving the determination of the next-to-leading order low-energy constant L^r_{10} from NNLO analyses of the flavor *ud* $V-A$ correlator is also highlighted.

DOI: 10.1103/PhysRevD.89.054036 PACS numbers: 12.39.Fe, 11.55.Hx, 13.35.Dx

I. INTRODUCTION

Chiral perturbation theory (ChPT) provides a means of implementing, in the most general way, the constraints on low-energy processes of the symmetries of QCD [1–3]. The effects of resonances, and other heavy degrees of freedom, are encoded in the low-energy constants (LECs) which appear in the resulting effective chiral Lagrangian multiplying those operators allowed by these constraints. In the even-intrinsic-parity sector, at next-to-leading order (NLO) in the chiral counting, the $SU(3)\times SU(3)$ Lagrangian involves ten in-principle measurable LECs, the L_k introduced in Ref. [3]. The next-to-next-to-leading order (NNLO) form was first considered in Ref. [4], and a reduced minimal set of operators subsequently found in Ref. [5]. The minimal NNLO $SU(3)$ form involves 94 additional LECs, 4 in contact and 90 in noncontact terms. In what follows, we work with the dimensionful versions, C_k, of the NNLO LECs introduced in Ref. [5].

To make the NNLO chiral Lagrangian fully predictive, existing determinations of the L_k must be supplemented with model-independent experimental and/or theoretical determinations of the C_k. To date, a limited number of such determinations exist.

First attempts at obtaining what is now called C_{61} were made in Refs. [6–8], with a more robust chiral sum rule determination, involving the flavor-breaking (FB) *ud-us* vector current correlator, obtained in Ref. [9]. C_{12} and the combination $C_{12}+C_{34}$ were determined via phenomenological [10,11] and lattice [12] analyses of the scalar $K\pi$ form factor, and $C_{14}+C_{15}$ and $C_{15}+2C_{17}$ from analyses of the quark-mass dependence of lattice data for f_K/f_π [12–14] (some aspects of these latter analyses employing, in addition, large-N_c arguments). Generally less precise constraints on the combinations $C_{88}-C_{90}$, $2C_{63}-C_{65}$ and $6C_{12}+2C_{63}+2C_{65}+3C_{90}$ were obtained from analyses of the charged π and K electromagnetic form factors [15], and on the combinations $C_{12}+2C_{13}$, C_{13} and $C_{12}+4C_{13}$ from analyses of the curvature of the π and strangeness-changing $K\pi$ scalar form factors [16]. An overconstrained (but, with current data, not yet fully self-consistent) determination of the set C_{1-4} was also made [17], using a combination of four of the subthreshold coefficients of the πK scattering amplitudes determined in Ref. [18] and two of the low-energy $\pi\pi$ scattering parameters determined in Ref. [19]. The four remaining $\pi\pi$ scattering parameters and six remaining πK subthreshold coefficients provide ten additional constraints on the 24 NNLO LECs C_{5-8}, C_{10-17}, C_{19-23}, C_{25}, C_{26} and C_{28-32} [17]. Finally, C_{87} has been determined from analyses of the light-quark V-A current-current correlator [20,21].

In the absence of clean theoretical and/or data-based determinations, it is common to use estimates of the C_k

[*]maarten@stars.sfsu.edu
[†]kmaltman@yorku.ca
[‡]Also at CSSM, University of Adelaide, Adelaide, South Australia 5005, Australia.
[§]peris@ifae.es

obtained in model-dependent approaches. One such strategy is to extend the resonance ChPT (RChPT) approach [22] (often held to work well in estimating NLO LECs [23]) to NNLO [24]. This approach typically employs, in addition to long-distance chiral constraints, short-distance QCD and large-N_c constraints. Evidence exists that at least some $1/N_c$-suppressed LECs cannot be neglected [25,26] (we will comment below on another such piece of evidence). A second approach to estimating the C_k, in a large-N_c gauge-invariant nonlocal quark model framework, was presented in Ref. [27]. Comparisons performed in Refs. [17,27] between predicted C_k values and those known from experiment expose some shortcomings in both approaches.

In light of this situation, additional model-independent NNLO LEC determinations are of interest, first as part of the ongoing long-term program of pinning down the parameters of the low-energy effective Lagrangian, and second, as a means of further testing, and constraining, models used to estimate additional as-yet-undetermined LECs. In this paper, we update the earlier determination of C_{61} [9] and provide a new high-precision determination of the combination $C_{12}+C_{61}+C_{80}$. With input for C_{12} from other sources (such as those noted above), this yields also a determination of C_{80}. A direct determination of the combination $C_{12}-C_{61}+C_{80}$, which, with the $1/N_c$-suppressed combination $C_{13}-C_{62}+C_{81}$, is needed to complete the determination of the NLO LEC L_{10} from an NNLO analysis of the low-energy behavior of the light quark V-A correlator [20,21], is also obtained. Combining this determination with the continuum light-quark V-A correlator analysis of Ref. [21] and the lattice analysis of Ref. [28] turns out to make possible a high-precision ($\sim$10%) determination of L_{10}. This level of precision requires careful consideration of the LEC combination $C_{13}-C_{62}+C_{81}$, which, though nominally subleading in $1/N_c$, turns out to have a nonzero value comparable to that of the non-$1/N_c$-suppressed combination $C_{12}-C_{61}+C_{80}$ (although with large errors) [21]. This nonzero value has a nontrivial impact on the determination of L_{10}, shifting the magnitude of the result by 15% compared to what is obtained if $C_{13}-C_{62}+C_{81}$ is instead set to zero on the grounds of its $1/N_c$ suppression [28].

The rest of the paper is organized as follows: In Sec. II, we introduce and give the explicit forms of the chiral sum rules to be employed. In Sec. III, the experimental, NLO LEC, and OPE inputs to these sum rules are specified. Section IV contains the results and a comparison to model predictions for the LEC combinations in question. Section V, finally, contains a brief summary. Details of the OPE contributions and errors are gathered in the Appendix.

II. THE FLAVOR-BREAKING CHIRAL SUM RULES

The key objects for the analysis described in this paper are the flavor $ij=ud$, us vector (V) and axial vector (A) current-current two-point functions, $\Pi^{\mu\nu}_{V/A}$, and their spin $J=0$, 1 components, $\Pi^{(J)}_{ij;V/A}$. These are defined by

$$\Pi^{\mu\nu}_{ij;V/A}(q^2)\equiv i\int d^4x e^{iq\cdot x}\langle 0|T(J^{\mu}_{ij;V/A}(x)J^{\dagger\nu}_{ij;V/A}(0))|0\rangle = (q^\mu q^\nu - q^2 g^{\mu\nu})\Pi^{(1)}_{ij;V/A}(Q^2)+q^\mu q^\nu \Pi^{(0)}_{ij;V/A}(Q^2), \tag{1}$$

where $J_{ij;V/A}$ are the standard flavor ij V/A currents, and $Q^2=-q^2=-s$. $\Pi^{(0,1)}_{ij;A}$ individually have kinematic singularities at $Q^2=0$, but their sum, $\Pi^{(0+1)}_{ij;A}$, and $s\Pi^{(0)}_{ij;A}$ are both kinematic singularity free. The associated spectral functions, $\rho^{(J)}_{ij;V/A}(s)=\mathrm{Im}\,\Pi^{(J)}_{ij;V/A}(s)/\pi$, are accessible experimentally through the normalized differential distributions, $dR_{ij;V/A}/ds$,

$$R_{ij;V/A}\equiv \Gamma[\tau^-\to\nu_\tau \mathrm{hadrons}_{ij;V/A}(\gamma)]/\Gamma[\tau^-\to\nu_\tau e^-\bar{\nu}_e(\gamma)], \tag{2}$$

measured in flavor ij V- or A-current-induced hadronic τ decays. Explicitly [29],

$$\frac{dR_{ij;V/A}}{ds}=\frac{12\pi^2|V_{ij}|^2 S_{\mathrm{EW}}}{m_\tau^2}\times[w_\tau(y_\tau)\rho^{(0+1)}_{ij;V/A}(s)-w_L(y_\tau)\rho^{(0)}_{ij;V/A}(s)], \tag{3}$$

with $y_\tau=s/m_\tau^2$, $w_\tau(y)=(1-y)^2(1+2y)$, $w_L(y)=2y(1-y)^2$, S_{EW} a known short-distance electroweak correction [30], and V_{ij} the flavor ij CKM matrix element. The dominant contributions to $\rho^{(0)}_{ud,us;A}(s)$ are the accurately known, chirally unsuppressed π and K pole terms. The remaining $J=0$ V/A spectral contributions are proportional to $(m_i\mp m_j)^2$, and hence numerically negligible for $ij=ud$. $\rho^{(0+1)}_{ud;V+A}(s)$ is thus determinable directly from the nonstrange differential decay distribution. For $ij=us$, phenomenological determinations strongly constrained by the known strange quark mass are available for the small continuum scalar $\rho^{(0)}_{us;V}(s)$ [31] and pseudoscalar $\rho^{(0)}_{us;A}(s)$ [32] contributions in the region $s<m_\tau^2$ relevant to hadronic τ decays. With the contributions proportional to $w_L(y_\tau)\rho^{(0)}_{us;V/A}(s)$ in Eq. (3) thus fixed, $\rho^{(0+1)}_{us;V+A}(s)$ can be determined from the strange differential decay distribution. The V/A separation for the ud and us cases will be discussed further in the next section.

Given a correlator, $\Pi(Q^2=-s)$, free of kinematic singularities, and the corresponding spectral function, $\rho(s)$, application of Cauchy's theorem to the contour shown in Fig. 1 yields the inverse-moment (chiral) finite-energy sum rule (IMFESR) relation, valid for any

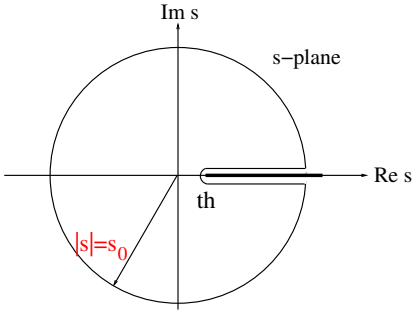

FIG. 1 (color online). The contour underlying the chiral sum rules of Eq. (4).

choice of weight function, $w(s)$, analytic in the region of the contour:

$$w(0)\Pi(0) = \frac{1}{2\pi i}\oint_{|s|=s_0} ds \frac{w(s)}{s}\Pi(Q^2) + \int_{th}^{s_0} ds \frac{w(s)}{s}\rho(s), \tag{4}$$

where th is the relevant physical threshold. We will work below with values of s_0 and FB correlator combinations, $\Pi(Q^2)$, such that the $\rho(s)$ needed on the rhs are accessible from hadronic τ-decay data. A determination of the combination of LECs occurring in the chiral representation of $\Pi(0)$ is then obtained by inputting the chiral representation on the lhs and evaluating both terms on the rhs. For large enough s_0, the first term on the rhs can be evaluated using the OPE representation of $\Pi(Q^2)$, while, for $s_0 < m_\tau^2$, the second term can be evaluated using experimental spectral data. Previous sum rule studies have, however, found that, even for $s_0 \sim 2$–3 GeV^2, integrated duality violations (OPE breakdown) can be sizeable for $w(s)$ which are not zero at the timelike point $s = s_0$ on the contour [33–35]. We thus further restrict our attention to $w(s)$ satisfying $w(s_0) = 0$.

We will consider two choices for the weight $w(y)$, $y = s/s_0$:

$$\begin{aligned} w_{DK}(y) &= (1-y)^3\left(1 + y + \frac{1}{2}y^2\right) \\ &= 1 - 2y + \frac{1}{2}[y^2 + y^3 + y^4 - y^5], \\ \hat{w}(y) &= (1-y)^3. \end{aligned} \tag{5}$$

The first of these was considered in Ref. [9]. Both weights satisfy $w(0) = 1$ and are "triply pinched" (i.e., they have a triple zero at $s = s_0$), strongly suppressing duality-violating contributions to the first term on the rhs of Eq. (4). An additional advantage of the triple zero is the suppression of contributions to the weighted spectral integrals [the second term on the rhs of Eq. (4)] from the high-s part of the spectral functions, where the us data currently available suffers from low statistics and large V/A-separation uncertainties [9]. The strong suppression at large s for these weights is thus doubly beneficial to the goal of this article, which is to determine as accurately as possible the lhs's, $w(0)\Pi(0) = \Pi(0)$, of Eq. (4) for various FB combinations, Π, of the ud and us V and A correlators [see Eq. (6) below].[1]

The value of $\Pi(0)$ in Eq. (4) should, of course, be independent both of s_0 and the choice of weight, $w(s)$. Verifying that these independences are in fact realized provides nontrivial tests of the self-consistency of the theoretical and spectral input to the analysis.

In the rest of the paper, we concentrate on IMFESRs involving one of the three choices, $T = V$, $V \pm A$, of the FB ud-us combinations of $J = 0 + 1$ V and A correlators,

$$\Delta\Pi_T \equiv \Pi^{(0+1)}_{ud;T} - \Pi^{(0+1)}_{us;T}. \tag{6}$$

The corresponding spectral functions are denoted $\Delta\rho_T$. Versions of the $T = V \pm A$ correlator and spectral-function combinations having their π and K pole contributions subtracted will be denoted by $\Delta\bar{\Pi}_{V\pm A}$ and $\Delta\bar{\rho}_{V\pm A}$. The restriction to the $J = 0 + 1$ combination is predicated on the very bad behavior of the OPE representation of $\Pi^{(0)}_{ij;V/A}(Q^2)$ on the contour $|Q^2| = s_0$ for all s_0 accessible using τ decay data [36,37].

It is worth commenting on the differences in the OPE contributions for the two weights w_{DK} and $\hat{w}$. We focus here on $D \geq 4$ contributions ($D = 2$ contributions will be discussed in more detail later, as will $D = 4$ contributions higher order in α_s). For a general polynomial $w(y) = \sum_{m=0} a_m y^m$, writing $[\Delta\Pi_T(Q^2)]^{OPE}_{D\geq 4}$ in the form $\sum_{k\geq 2} C^T_{2k}/Q^{2k}$, with C^T_D an effective dimension-D

[1]The motivation for the choice of weights here is to be contrasted with that in Refs. [34,35], in which the principal aim was a precision determination of $\alpha_s(m_\tau^2)$ from the non-FB ud V and A correlators. The need for high ($\sim$1% or less) precision on the theoretical side of the sum rules employed in that case favors a restriction to weights of lower degree, which minimize the number of $D \geq 6$ OPE condensates that need to be fit to data, but have less pinching than those in the present case. As the level of pinching decreases, the possibility for significant integrated duality violations increases. As explained in detail in Ref. [34], the inclusion of unpinched weights in that analysis allowed for the modeling and constraining of these contributions, providing a means for investigating quantitatively the level of integrated duality violation not only in that case but also in earlier pinched-weight analyses. Here, the situation is different, as the use of triply pinched polynomials $w(y)$ in the full weights, $w(y)/s$, used to access the low-s physics of interest to us, not only strongly suppresses duality-violating contributions, as already noted above, but also significantly reduces the errors on the weighted us spectral integrals. The additional $1/s$ factor in the weights further helps by reducing the maximum dimension of OPE condensates which have to be considered in the analysis. The final important difference between the present case and that of the α_s analysis is the precision required for the OPE contributions. Here, OPE contributions turn out to play a smaller numerical role, greatly reducing the level of precision required for the evaluation of these contributions.

condensate, the integrated $D \geq 4$ OPE contributions to the rhs of Eq. (4) become

$$\frac{1}{2\pi i}\oint_{|s|=s_0} ds \frac{w(s/s_0)}{s}[\Delta\Pi_T(Q^2)]^{OPE}_{D\geq 4} = \sum_{k\geq 2}(-1)^k a_k \frac{C^T_{2k}}{s_0^k} \tag{7}$$

up to logarithmic corrections suppressed by additional powers of α_s. Since $\hat{w}$ has degree 3, only OPE contributions up to $D = 6$ contribute, if we ignore the α_s-suppressed logarithmic corrections. In contrast, w_{DK}, which has degree 5, produces contributions at leading order in α_s up to $D = 10$. In this sense, $\hat{w}$ is preferred over w_{DK}, since the latter involves additional unknown or poorly known $D = 8$ and $D = 10$ condensates. For w_{DK}, these contributions are expected to be small, partly because the coefficients a_m, $m = 4, 5$ are small enough to avoid unwanted enhancements, and partly because of the $1/s_0^{D/2}$ suppression of such higher-D contributions for $s_0 \gg \Lambda^2_{QCD}$, but this expectation can (and should) be tested. Performing the IMFESR analysis for a range of s_0 provides a means of doing so and, in fact, provides a test of the reliability of any approximations employed in evaluating the rhs, including also the neglect of integrated duality violations. The s_0 dependence of the rhs of Eq. (4) will be considered for the combinations of Eq. (6) for both weights in Sec. IV below.

An advantage of the weight w_{DK} over $\hat{w}$ is that the $D = 2, 4$ contributions to the integral in Eq. (7) are better behaved for w_{DK}. In addition, as can be seen from Eq. (7), since $a_2^{\hat{w}}/a_2^{w_{DK}} = 6$, the leading-order $D = 4$ contribution, and the associated error are both a factor of $\sim$6 larger for $\hat{w}$. Analogous, though somewhat smaller, enhancement factors, $|a_1^{\hat{w}}/a_1^{w_{DK}}| = 3/2$ and $|a_3^{\hat{w}}/a_3^{w_{DK}}| = 2$ are operative for the leading-order $\hat{w}$ $D = 2$ and $D = 6$ contributions and errors. $D = 2, 4$ and 6 contributions, and hence total OPE errors, are thus significantly larger for $\hat{w}$ than for w_{DK} from this effect alone. The nominal convergence of the known terms in the integrated $D = 2$ OPE series is also significantly slower for $\hat{w}$. The larger OPE errors turn out to produce total errors for $\hat{w}$ which are similar to those for w_{DK} (cf. Table II in Sec. IV). The differences in the relative sizes of spectral integral and OPE contributions to the rhs's of the w_{DK} and $\hat{w}$ IMFESRs also means that the tests of self-consistency provided by the agreement of the results of the two analyses are indeed nontrivial.

Below, the magnitude of the $D = 6$ contributions will be estimated using the vacuum saturation approximation (VSA) with very generous errors, and $D = 8$ and $D = 10$ contributions will be assumed negligible.[2] The fact that higher-D contributions vary more strongly with s_0 than do integrated lower-dimensional $D = 2$, 4 contributions means that these assumptions can also be tested, provided a range of s_0 is employed in the analysis. As already emphasized above, such s_0-stability tests play an important role in all such sum-rule analyses.

For $T = V \pm A$, π and K pole contributions appear on both sides of Eq. (4). The LECs of interest in these cases, in fact, appear only in the pole-subtracted parts, $\Delta\bar{\Pi}_{V\pm A}$, of the $\Delta\Pi_{V\pm A}$, and it is thus convenient to move all the pole contributions to the corresponding rhs's. With $w_{DK}(0) = \hat{w}(0) = 1$, the three IMFESRs of interest, for $w(s) = w_{DK}(y)$ or $\hat{w}(y)$, then take the form

$$\Delta\Pi_V(0) = \frac{1}{2\pi i}\oint_{|s|=s_0} ds \frac{w(s)}{s}[\Delta\Pi_V(Q^2)]^{OPE} + \int_{th}^{s_0} ds \frac{w(s)}{s}\Delta\rho_V(s), \tag{8}$$

$$\Delta\bar{\Pi}_{V\pm A}(0) = \frac{1}{2\pi i}\oint_{|s|=s_0} ds \frac{w(s)}{s}[\Delta\Pi_{V\pm A}(Q^2)]^{OPE} + \int_{th}^{s_0} ds \frac{w(s)}{s}\Delta\bar{\rho}_{V\pm A}(s) \pm \left[\frac{f_K^2}{s_0} f^w_{\rm res}(y_K) - \frac{f_\pi^2}{s_0} f^w_{\rm res}(y_\pi)\right], \tag{9}$$

where, owing to the pole subtraction, th is now the continuum threshold $4m_\pi^2$, $y_\pi = m_\pi^2/s_0$, $y_K = m_K^2/s_0$, $f^{w_{DK}}_{\rm res}(y) = 4 - y - y^2 - y^3 + y^4$ and $f^{\hat{w}}_{\rm res}(y) = 6 - 6y + 2y^2$. The normalization of the decay constants is such that $f_\pi \approx 92$ MeV. Note that it is the full correlators $\Delta\Pi_{V\pm A}$, including the π/K pole contributions, which occur in the first term of the rhs of Eq. (9). We discuss the inputs to the rhs's of Eqs. (8) and (9) in the next section.

We conclude this section with the NNLO low-energy representations of the lhs's of Eqs. (8) and (9). The general structure of these representations is $R^T(0) + [\Delta\Pi_T(0)]_{\rm LEC}$, with

$$[\Delta\Pi_T(0)]_{\rm LEC} = \sum_{k=5,9,10} c_k^T L_k^r + 32(m_K^2 - m_\pi^2)\sum_{k=12,61,80} a_k^T C_k^r, \tag{10}$$

and $R^T(0)$, the NLO LECs L_k^r and the NNLO LECs C_k^r all depending on the chiral renormalization scale μ. The $R^T(0)$'s combine all one- and two-loop contributions involving only LO vertices, and are completely fixed by the pseudoscalar meson masses, decay constants and μ. Their forms are rather lengthy (especially for the $T = V \pm A$ cases) and hence not presented here. They can be reconstructed from the results of Secs. 4, 6 and Appendix B of Ref. [38]. NLO contributions proportional to the L_k^r cancel in the FB combinations considered here. The

[2]Existing fits for the effective $D = 6$ and 8 condensates, $C_{6,8}$, for the ud V and A correlators can be used to evaluate the ud contributions to the FB $D = 6 + 8$ differences. These results will be used as a very conservative bound for the corresponding FB combinations.

coefficients $c^T_{5,9,10}$ are generated by one-loop graphs with a single NLO vertex, and thus also μ dependent. The a^T_k are, in contrast, μ independent at this order.

Fixing the chiral scale μ to the conventional scale choice $\mu_0 \equiv 0.77$ GeV, the explicit forms of the $[\Delta\Pi_T(0)]_{\rm LEC}$ become

$$\begin{aligned}
[\Delta\Pi_V(0)]_{\rm LEC} &= -0.7218L^r_5 + 1.423L^r_9 + 1.062L^r_{10} \\
&\quad + 32(m_K^2 - m_\pi^2)C^r_{61}, \\
[\Delta\bar{\Pi}_{V+A}(0)]_{\rm LEC} &= -0.7218L^r_5 + 1.423L^r_9 \\
&\quad + 32(m_K^2 - m_\pi^2)[C^r_{12} + C^r_{61} + C^r_{80}], \\
[\Delta\bar{\Pi}_{V-A}(0)]_{\rm LEC} &= -0.7218L^r_5 + 1.423L^r_9 + 2.125L^r_{10} \\
&\quad - 32(m_K^2 - m_\pi^2)[C^r_{12} - C^r_{61} + C^r_{80}], \quad (11)
\end{aligned}$$

where the renormalized LECs are all understood to be evaluated at $\mu = \mu_0$, and m_π and m_K have been taken to be the charged pion mass and, for definiteness, the average of the charged and neutral kaon masses. (Taking instead m_K to be the charged K mass has no impact on our final results.) The corresponding values for the LEC-independent R_T contributions are

$$\begin{aligned}
R_V(\mu_0) &= 0.00775, \\
R_{V+A}(\mu_0) &= 0.00880, \\
R_{V-A}(\mu_0) &= 0.00670. \quad (12)
\end{aligned}$$

III. INPUTS TO THE V, $V+A$ AND $V-A$ IMFESRS

A. Meson masses, decay constants and NLO LEC inputs

PDG 2012 values [39] are used for f_π, m_π, m_K and m_η (the latter is required in evaluating some of the NNLO contributions). Explicitly, $m_\pi = 139.57$ MeV, $m_\eta = 547.85$ MeV and $m_K = 495.65$ MeV, the latter being the average of the charged and neutral masses. For the normalization used here, $f_\pi = 92.21(14)$ MeV [39]. f_K is obtained by combining this value with the current FLAG assessment of $n_f = 2+1$ lattice results, $f_K/f_\pi = 1.193(5)$ [40].

The NNLO representation of $\Delta\bar{\Pi}_{V+A}(0)$ does not involve L^r_{10}, so the only NLO LECs required as input to the determination of the corresponding NNLO LEC combination $C^r_{12} + C^r_{61} + C^r_{80}$ are L^r_5 and L^r_9. The $\Delta\Pi_V(0)$ and $\Delta\bar{\Pi}_{V-A}(0)$ IMFESRs, in contrast, also require input on L^r_{10}.

For L^r_5 and L^r_9, we employ the values $L^r_5(\mu_0) = 0.00058(13)$ and $L^r_9(\mu_0) = 0.00593(43)$. The former is the result of the recommended *All* fit from the most recent NNLO analysis of the NLO LECs L^r_{1-8}, given in Table 5 of Ref. [26]. The latter was obtained in an NNLO analysis of the π and K electromagnetic form factors [15]. The contributions proportional to L^r_5 in the three IMFESRs under consideration are numerically rather small, and the resulting contributions to the errors on the corresponding NNLO LEC combinations negligible in comparison to the contributions from other sources.

The situation with L^r_{10} is somewhat more complicated, since the NNLO determination of L^r_{10} is not independent of the NNLO LECs appearing in the $\Delta\Pi_V$ and $\Delta\bar{\Pi}_{V-A}$ IMFESRs. The standard route to an experimental determination of L^r_{10} has been through a dispersive or IMFESR determination of the value of the π-pole-subtracted light-quark V-A correlator, $\bar{\Pi}_{ud;V-A}(Q^2)$, at $Q^2 = 0$. An early IMFESR analysis, employing ChPT to NLO may be found in Ref. [41]. Two NLO determinations using lattice data for $\Pi_{ud;V-A}(Q^2)$ also exist [42,43]. A very precise determination,

$$\bar{\Pi}_{ud;V-A}(0) = 0.0516(7), \quad (13)$$

has been obtained in Ref. [21] using the results of Refs. [34,35] in combination with the updated version of the OPAL nonstrange spectral distributions [44] reported in Ref. [35]. A similar result for $\Pi_{ud;V-A}(0)$ has been obtained in Ref. [20] using the nonstrange ALEPH rather than OPAL data [45]. The error on the result of Ref. [20] is, unfortunately, not reliable, owing to an error in the publicly posted covariance matrices for the version of the ALEPH data used in that analysis [46].

It is now known that the NLO approximation provides a very poor representation of the low-Q^2 dependence of $\bar{\Pi}_{ud;V-A}(Q^2)$ [21]. This result, which is not unexpected in view of a similar observation about the NLO representation of the ud V correlator [47], clearly calls into question the results for L^r_{10} obtained from NLO analyses.

The NNLO representation of $\bar{\Pi}_{ud;V-A}(0)$ required to extend the NLO analyses to NNLO has the form [38]

$$\bar{\Pi}_{ud;V-A}(0) = \mathcal{R}_{ud;V-A} + \hat{c}_9 L^r_9 + \hat{c}_{10} L^r_{10} + \mathcal{C}^r_0 + \mathcal{C}^r_1, \quad (14)$$

where $\mathcal{R}_{ud;V-A}$ is the sum of one- and two-loop contributions involving only LO vertices,

$$\begin{aligned}
\hat{c}_9 &= 16(2\mu_\pi + \mu_K), \\
\hat{c}_{10} &= -8(1 - 8\mu_\pi - 4\mu_K), \quad (15)
\end{aligned}$$

with $\mu_P = \frac{m_P^2}{32\pi^2 f_\pi^2}\log(\frac{m_P^2}{\mu^2})$ being the usual chiral logarithm, and

$$\begin{aligned}
\mathcal{C}^r_0 &= 32m_\pi^2[C^r_{12} - C^r_{61} + C^r_{80}], \\
\mathcal{C}^r_1 &= 32(m_\pi^2 + 2m_K^2)[C^r_{13} - C^r_{62} + C^r_{81}]. \quad (16)
\end{aligned}$$

$\mathcal{R}_{ud;V-A}$, $\hat{c}_9$ and $\hat{c}_{10}$ are all fixed by the chiral scale μ and pseudoscalar masses and decay constants. The NNLO LECs appearing in $\mathcal{C}^r_0$ are LO in $1/N_c$, and those in $\mathcal{C}^r_1$ are $1/N_C$ suppressed. Note that $\mathcal{C}^r_0$ involves precisely the combination of NNLO LECs appearing in $\Delta\bar{\Pi}_{V-A}(0)$. For

$\mu = \mu_0$, the results of Ref. [21] for $\bar{\Pi}_{ud;V-A}(0)$ and Ref. [15] for $L_9^r(\mu_0)$ yield the very precise constraint

$$L_{10}^r(\mu_0) = -0.004098(59)_{exp}(74)_{L_9^r} + 0.0822(\mathcal{C}_0^r + \mathcal{C}_1^r) \tag{17}$$

on $L_{10}^r(\mu_0)$, $\mathcal{C}_0^r(\mu_0)$ and $\mathcal{C}_1^r(\mu_0)$.[3] Information on $\mathcal{C}_0^r(\mu_0)$ and $\mathcal{C}_1^r(\mu_0)$ is, however, required to turn this into a determination of $L_{10}^r(\mu_0)$. The differing dependences of $\hat{c}_9$, $\hat{c}_{10}$, $\mathcal{C}_0^r$ and $\mathcal{C}_1^r$ on the meson masses makes it natural to approach this problem using the lattice, where the pseudoscalar meson masses can be varied by varying the input quark masses.

Such an analysis has been carried out in Ref. [28]. The first stage of this analysis uses lattice and continuum data for $\bar{\Pi}_{ud;V-A}(Q^2)$ in combination with the constraint, Eq. (17), obtained from the already published result for $\bar{\Pi}_{ud;V-A}(0)$, Eq. (13). For low Euclidean Q^2, the errors on the lattice data for $\bar{\Pi}_{ud;V-A}(Q^2)$ are currently larger than those on the continuum version. The consequence is that, while use of the lattice data in combination with the $\bar{\Pi}_{ud;V-A}(0)$ constraint, Eq. (17), *does* allow all three of L_{10}^r, $\mathcal{C}_0^r$ and $\mathcal{C}_1^r$ to be determined, the errors that result from this first-stage analysis are at the ∼25%, ∼100% and ∼80% levels for L_{10}^r, $\mathcal{C}_0^r$ and $\mathcal{C}_1^r$, respectively. The $\Delta\bar{\Pi}_{V-A}$ IMFESR, which involves a distinct combination of two of these three quantities, L_{10}^r and $\mathcal{C}_0^r$, provides an additional constraint, and allows an extended (second-stage) version of the analysis of Ref. [28] to be carried out. The extended analysis, which employs our results below for the $\Delta\bar{\Pi}_{V-A}$ IMFESR constraint as input, produces results [quoted in Eqs. (27), (28) and (29) below] with significantly reduced errors.

In presenting the results of the IMFESR analyses below, we will thus first quote the result for $C_{12}^r + C_{61}^r + C_{80}^r$ from the $\Delta\bar{\Pi}_{V+A}$ IMFSER, which is independent of the treatment of L_{10}^r, and then quote the result for the constraint on L_{10}^r and $\mathcal{C}_0^r$ arising from the $\Delta\bar{\Pi}_{V-A}$ IMFESR. The $\Delta\bar{\Pi}_{V+A}$ and $\Delta\bar{\Pi}_{V-A}$ IMFESRs can, of course, also be combined to obtain the related (but not independent) $\Delta\Pi_V$ and $\Delta\bar{\Pi}_A$ IMFESRs. The former constrains the combination of L_{10}^r and C_{61}^r noted above; the latter an analogous combination of L_{10}^r and $C_{12}^r + C_{80}^r$. To go further, and turn these constraints into explicit determinations of the corresponding NNLO LEC combinations, requires input on L_{10}^r. We will employ for L_{10}^r the result of the second-stage combined lattice-continuum analysis of Ref. [28]. This analysis incorporates the $w_{DK}(y)$ version of the $\Delta\bar{\Pi}_{V-A}$ IMFESR constraint, in addition to the $\bar{\Pi}_{ud;V-A}(0)$ constraint, Eq. (17), and the constraints generated by data from four different lattice ensembles. The resulting error for L_{10}^r is dominated by lattice errors, and hence independent of those in the present analysis. With this input for L_{10}^r, C_{61}^r follows from the $\Delta\Pi_V$ IMFESR constraint and $C_{12}^r + C_{80}^r$ from the $\Delta\bar{\Pi}_A$ IMFESR constraint. External input on C_{12}^r then allows us to also fix C_{80}^r.

B. OPE input

The correlator combinations entering the IMFESRs under consideration are all flavor breaking and thus have vanishing $D = 0$ OPE series. We include $D = 2$ and 4 contributions for all channels, treat $D = 6$ and 8 contributions as discussed below, and assume that $D = 10$ and higher contributions can be neglected for IMFESRs based on either $w_{DK}(y)$ or $\hat{w}(y)$. Integrated duality violations will also be neglected. Since integrated OPE contributions of $D = 2k$ scale, up to logarithms, as $1/s_0^k$ [see Eq. (7)], and integrated duality violations typically produce contributions with oscillatory s_0-dependence, these assumptions can be tested by studying the IMFESRs [Eqs. (8) and (9)] over a range of s_0 and ensuring that the resulting $Q^2 = 0$ correlator values are independent of s_0, as well as of the choice of weight, as they should be.

The $D = 2$ OPE series for the flavor $ij = ud$, us, $J = 0 + 1$, V and A correlators are known to four loops. The explicit expressions to three loops, including light-quark mass corrections, may be found in Ref. [48], and the $O(m_s^2)$ terms in the four-loop contributions in Ref. [49]. Expressions for the corresponding $D = 4$ and 6 contributions may be found in Refs. [50,51].

Omitting, for presentational simplicity, corrections suppressed by 1 or more powers of $m_{u,d}/m_s$, these results imply, for $D = 2$,

$$\begin{aligned}
[\Delta\Pi_V(Q^2)]_{D=2}^{OPE} &= \frac{3}{4\pi^2}\frac{m_s^2(Q^2)}{Q^2}\left[1 + \frac{7}{3}\bar{a} + 19.9332\bar{a}^2 + 208.746\bar{a}^3 + \cdots\right],\\
[\Delta\Pi_{V+A}(Q^2)]_{D=2}^{OPE} &= \frac{3}{2\pi^2}\frac{m_s^2(Q^2)}{Q^2}\left[1 + \frac{7}{3}\bar{a} + 19.9332\bar{a}^2 + 208.746\bar{a}^3 + \cdots\right],\\
[\Delta\Pi_{V-A}(Q^2)]_{D=2}^{OPE} &= \frac{3}{2\pi^2}\frac{m_u(Q^2)m_s(Q^2)}{Q^2}\left[\frac{2}{3}\bar{a} + 8.7668\bar{a}^2 + \cdots\right],
\end{aligned} \tag{18}$$

[3]The slight difference between the result given in Eq. (17) and that quoted in Eq. (4.9) of Ref. [21], $L_{10}^r = -0.004113(89)_{exp}(74)_{L_9^r}$, results from the inadvertent use in Ref. [21] of the less precise determination of the quantity $L_{10}^{\rm eff}$, given by Eq. (4.1) of that reference, in place of the most precise determination, Eq. (4.2 b). Switching instead to the most precise determination, Eq. (4.2 b), leads to the result quoted in Eq. (17).

where $\bar{a} \equiv \alpha_s(Q^2)/\pi$, with $\alpha_s(Q^2)$ being the $\bar{M}S$ running coupling, and $m_u(Q^2)$ and $m_s(Q^2)$ are the $\bar{M}S$ running u and s quark masses.

For $D = 4$, one has, omitting numerically negligible contributions of fourth order in the quark masses and terms suppressed by $m_{u,d}/m_s$,

$$
\begin{aligned}
[\Delta\Pi_V(Q^2)]^{OPE}_{D=4} &= -\frac{1}{Q^4}\left(\frac{m_s}{\hat{m}}\right)\langle \hat{m}\,\bar{u}\,u\rangle \\
&\quad \times \left[r_c + \bar{a}\left(\frac{4}{3} - r_c\right) + \bar{a}^2\left(\frac{59}{6} - \frac{13}{3}r_c\right)\right], \\
[\Delta\Pi_{V+A}(Q^2)]^{OPE}_{D=4} &= -\frac{2}{Q^4}\left(\frac{m_s}{\hat{m}}\right) r_c\langle \hat{m}\,\bar{u}\,u\rangle\left[1 - \bar{a} - \frac{13}{3}\bar{a}^2\right], \\
[\Delta\Pi_{V-A}(Q^2)]^{OPE}_{D=4} &= -\frac{1}{Q^4}\left(\frac{m_s}{\hat{m}}\right)\langle \hat{m}\,\bar{u}\,u\rangle\left[\frac{8}{3}\bar{a} + \frac{59}{3}\bar{a}^2\right], \quad (19)
\end{aligned}
$$

where $\hat{m} = (m_u + m_d)/2$ and $r_c = \langle \bar{s}s\rangle/\langle \bar{u}u\rangle$.

$D = 6$ contributions are expected to be dominated by contributions from four-quark condensates. These condensates are not known experimentally for the flavor us correlators but can be roughly estimated using the VSA. In this approximation, one has [51]

$$
\begin{aligned}
&[\Pi^{(0+1)}_{ij;V/A}(Q^2)]^{OPE}_{D=6,VSA} \\
&\quad = \frac{32\pi}{81}\frac{\alpha_s}{Q^6}[\mp 9\langle \bar{q}_i q_i\rangle\langle \bar{q}_j q_j\rangle + \langle \bar{q}_i q_i\rangle^2 + \langle \bar{q}_j q_j\rangle^2], \quad (20)
\end{aligned}
$$

from which the VSA approximations to $[\Delta\Pi_V]^{OPE}_{D=6}$ and $[\Delta\Pi_{V\pm A}]^{OPE}_{D=6}$ are easily obtained. With these estimates, one finds that $D = 6$ contributions are numerically very small, particularly so for the V and $V + A$ IMFESRs, where they could be safely neglected even if the VSA were to be in error by an order of magnitude.[4]

The VSA estimates for the $D = 6$ contributions to the FB IMFESRs, being proportional to the FB factor $r_c - 1$, display quite strong cancellations. Some care must thus be exercised in assigning errors to these estimates. Here it is possible to take advantage of recent results for the effective $D = 6$ and $D = 8$ condensates appearing in the OPE representations of $\Pi_{ud;V}$, $\Pi_{ud;A}$ and $\Pi_{ud;V-A}$, obtained in the course of the analyses described in Refs. [21,35]. These allow a determination of the sum of the $D = 6$ and 8 contributions to the ud parts of the relevant IMFESR OPE integrals. Although the corresponding flavor us contributions are not known, some degree of cancellation will certainly be present in the FB ud-us differences. The flavor ud $D = 6 + 8$ OPE sums can thus be used to provide a very conservative estimate of the uncertainties on the central FB ud-us $D = 6 + 8$ OPE contributions described above.

The inputs required to evaluate the $D = 2$, 4 OPE contributions are as follows: For the running coupling and masses, we employ the exact solutions generated using the four-loop-truncated β and γ functions [52]. The initial condition for α_s is taken to be $\alpha_s^{n_f=3}(m_\tau^2) = 0.3181(57)$, obtained from the $n_f = 5$ PDG 2012 assessment $\alpha_s(m_Z^2)^{n_f=5} = 0.1184(7)$ via standard four-loop running and three-loop matching at the flavor thresholds [53]. For the initial conditions for the running masses, we take the results for $m_{u,d,s}(2\ \text{GeV})$ contained in the latest FLAG assessment [40]. The GMOR relation $\hat{m}\langle \bar{u}u\rangle = -\frac{1}{2}m_\pi^2 f_\pi^2$ is used for the light-quark condensate. For the ratio of strange to light condensates, the recent lattice result, $r_c = 1.08(16)$ [54], is in good agreement with the value $r_c = 1.1(3)$ obtained by updating the sum-rule result of Ref. [55] for modern $n_f = 2 + 1$ values of the ratio f_{B_s}/f_B. To be conservative, we will take the larger of the two errors.

In the case of the V and $V + A$ IMFESRs, the largest source of uncertainty in the OPE contribution turns out to lie in the treatment of the integrated $D = 2$ series. Since $\alpha_s(m_\tau^2)/\pi \simeq 0.1$, one sees from Eqs. (18) that, in these cases, the convergence of the known terms in the $D = 2$ series is marginal at best: at the spacelike point on the contour, the four-loop $[O(\bar{a}^3)]$ $D = 2$ term in fact exceeds the three-loop $[O(\bar{a}^2)]$ one for all s_0 accessible using τ-decay data. The rather problematic convergence behavior of the $D = 2$ series manifests itself not only in a similarly problematic behavior for the integrated $D = 2$ series, but also in a large difference, increasing with truncation order, between the results of evaluations of the integrated truncated series obtained using the FOPT (fixed-order perturbation theory) and CIPT (contour-improved perturbation theory) prescriptions. The two prescriptions differ only by contributions of order higher than the truncation order, the former involving the truncation of the integrated series at fixed order in $\alpha_s(s_0)$, the latter the summation of logarithms point by point along the contour via the local scale choice $\mu^2 = Q^2$ and truncation at the same fixed order in $\alpha_s(Q^2)$ for all such Q^2.

The problematic convergence behavior and increase in the FOPT-CIPT difference with increasing truncation order both suggest the $D = 2$ series may already have begun to display its asymptotic character at three- or four-loop order, complicating an assessment of the error to be assigned to the integrated truncated series. This issue has been raised previously in the context of the determination of $|V_{us}|$ from FB hadronic τ decay sum rules [56].

Fortunately, the lattice provides a means of investigating the reliability of various treatments of the $D = 2$ OPE series. In Ref. [57], lattice data for the FB $V + A$ combination was shown to favor the fixed-scale over the local-scale treatment of the $D = 2$ series, and hence FOPT over CIPT for the IMFESR integrals. Moreover, with the

[4]In fact, the VSA turns out to yield central values for the $D = 6$ contributions much smaller than the corresponding estimated errors. To the number of digits quoted below, our final results are, in fact, unchanged if we shift from our VSA estimates to zero for the $D = 6$ contributions.

three-loop-truncated, fixed-scale version of the $D = 2$ series, the OPE was found to provide a good representation of the lattice data for Q^2 in the range from m_τ^2 down to ~ 2 GeV^2 [57]. In view of these results, the integrated $D = 2$ OPE contribution has been evaluated using the FOPT prescription truncated at three loops. The associated error is taken to be the quadrature sum of (i) the three-loop FOPT-CIPT difference, (ii) the magnitude of the last (three-loop) term retained in the integrated FOPT series, (iii) the error associated with the uncertainty in the input $m_s(2\text{ GeV})$, and (iv) the error associated with the uncertainty in the input $\alpha_s(m_\tau^2)$. The resulting error is dominated by the FOPT-CIPT difference for w_{DK}, while both the FOPT-CIPT difference and last-term-retained contributions are important for $\hat{w}$. Based on the lattice results, this approach should, in fact, yield a rather conservative assessment of the $D = 2$ error.

Further details of our assessments of the errors on the various OPE contributions may be found in the Appendix.

C. Flavor *ud* and *us* spectral input

The weighted spectral integrals needed to complete the evaluations of the rhs's of the IMFESRs in Eq. (9) are

$$\int_{th}^{s_0} ds \frac{w(s)}{s} \rho^{(0+1)}_{ud,us;V}(s) \quad \text{and} \quad \int_{th}^{s_0} ds \frac{w(s)}{s} \bar{\rho}^{(0+1)}_{ud,us;A}(s), \tag{21}$$

with $w(s) = w_{DK}(y)$ or $\hat{w}(y)$, and the range 2.15 GeV$^2 < s_0 < m_\tau^2$ (the lower bound reflecting the binning of the ALEPH data) employed to carry out the s_0-stability (self-consistency) tests noted above.

An update of the OPAL results for $\rho^{(0+1)}_{ud;V}(s)$ and $\bar{\rho}^{(0+1)}_{ud;A}(s)$ [44], reflecting changes to the exclusive-mode branching fractions since the original OPAL publication, was performed in Ref. [35]. This update employed non-strange branching fractions from an HFAG fit incorporating Standard Model expectations based on $\pi_{\mu 2}$ and $K_{\mu 2}$ decay widths and then-current strange branching fractions from the same fit. Since then, Belle has produced a new result for $B[\tau^- \to K_S\pi^-\pi^0\nu_\tau]$ [58] which shifts slightly the previous world average for this mode. To restore the sum over all branching fractions to 1 after this shift, and in the absence of an update of the previously used HFAG fit which takes this shift into account, a common global 0.99971 rescaling has been performed on the *ud* V and A distributions of Ref. [35]. Being so close to 1, this rescaling, not surprisingly, has negligible effect.

The V/A separation for the nonstrange modes was performed by OPAL using G parity. The main uncertainty in this separation results from $K\bar{K}\pi$ contributions, for which G parity cannot be used. A conservative, fully anticorrelated $50 \pm 50\%$ V/A breakdown was assumed. While the $K\bar{K}\pi$ V/A separation uncertainty can, in principle, be significantly reduced through angular analyses [59] of the much higher statistics B-factory data on these modes, such an improvement is irrelevant for our purposes, since this uncertainty plays a negligible role in the present analysis.

The differential decay distribution $dR_{us;V+A}/ds$ has been measured, and its exclusive mode contributions made available, by the ALEPH Collaboration [60]. Much higher statistics B-factory results now exist for the relative (unit-normalized) distributions of the $K^-\pi^0$ [61], $K_S\pi^-$ [62], $K^-\pi^+\pi^-$ [63,64] and $K_S\pi^-\pi^0$ [58] exclusive modes, the latter in preliminary form only. We employ the B-factory results for these four modes, using current branching fraction values to fix the overall normalizations.[5] For all other modes, the ALEPH results, rescaled to current branching fraction values, are used. The $J = 0$ subtraction of the $dR_{us;V+A}/ds$ distribution, required to extract the $J = 0 + 1$ component contribution thereof, and hence the combination $\bar{\rho}^{(0+1)}_{us;V+A}(s)$ is, as noted above, performed using the results of Refs. [31,32]. For $|V_{us}|$ (needed to convert from dR/ds to the spectral function), we employ the value 0.2255(10) implied by three-family unitarity and the Hardy-Towner determination $|V_{ud}| = 0.97425(22)$ [65].

The V/A separation of the us, $V + A$ distribution is more complicated than in the analogous ud case. While the K pole contribution is pure A, and the $K\pi$ distribution pure V, chirally unsuppressed V and A contributions are both present for all the higher-multiplicity $Kn\pi$ ($n \geq 2$) modes. For $K\pi\pi$, the V/A separation could be performed, up to small chirally suppressed corrections, by a relatively simple angular analysis [59], but this has yet to be done. Fortunately, for phase-space reasons, the $K\pi\pi$ and higher-multiplicity strange mode distributions lie at relatively high s, increasingly so with increasing multiplicity. Their contributions to the IMFESR spectral integrals are thus strongly suppressed by the combination of the $1/s$ factor in the overall weight, $w(s)/s$, and the triple zeros of $w_{DK}(y)$ and $\hat{w}(y)$ at $s = s_0$. The suppression of such high-s contributions, of course, grows stronger as s_0 is decreased. The strong high-s suppression is also welcome in view of the low statistics and consequent large errors for the high-s part of the ALEPH us distribution and the fact that the s dependences of the ALEPH $K3\pi$, $K\eta$, $K4\pi$ and $K5\pi$ distributions were fixed from Monte Carlo rather than by direct measurement. The high-s suppression is, in fact, strong enough to allow the analyses to proceed with a

[5]The version of the Belle $K_S\pi^-\pi^0$ results used here is preliminary, having been read off from Fig. 2 of the report, Ref. [58], prepared by the Belle Collaboration for the Tau 2012 proceedings. The errors take into account the uncertainty in the reported branching fraction in addition to those shown in the figure. While this should (and will) be updated once the final version of the Belle analysis is released, the $K_S\pi^-\pi^0$ uncertainties errors play a negligible role in the V and $V - A$ analyses (where they are swamped by the much larger V/A separation uncertainties) and a very small role in the $V + A$ analysis (where $K\pi$ error contributions are dominant). The preliminary nature of the Belle data should thus have no relevant impact on the present analysis.

$50 \pm 50\%$ (fully anticorrelated) V/A breakdown assigned to contributions from all modes other than K and $K\pi$.

As noted in Refs. [9,60], however, the $K\pi\pi$ distributions contain contributions from the axial $K_1(1270)$, the axial $K_1(1400)$ and the vector $K^*(1410)$ resonances. While the latter two cannot be disentangled without an angular analysis, the former lies in a distinct part of the spectrum and can be unambiguously assigned to the A channel. This observation allows an improvement to be made on the V/A separation for the $K\pi\pi$ modes. Dürr and Kambor [9], following ALEPH [60], modeled the $K\pi\pi$ distribution as a sum of two resonant contributions, one from the $K_1(1270)$ and one from a single effective 1400 region resonance with mass and width equal to the average of the corresponding $K_1(1400)$ and $K^*(1410)$ parameters. The resulting 1400 region contribution was then assigned $50 \pm 50\%$ each to the V and A channels. For the V channel considered by Dürr and Kambor, the resulting ALEPH-based $K\pi\pi$ IMFESR contribution was found to be only $\sim 5\%$ ($\sim 7\%$) of the corresponding $K\pi$ one at $s_0 \sim 2$ GeV^2 ($s_0 \sim m_\tau^2$).

This approximate separation of V and A contributions to the $K\pi\pi$ spectral distribution can be carried out even more convincingly with the much-higher-precision *BABAR* $K^-\pi^+\pi^-$ [64] and Belle $K_S\pi^-\pi^0$ [58] data, both presented at Tau 2012. Figure 2 shows the us spectral function contributions produced by these data sets. The $K_1(1270)$ peak is clearly visible for both modes. Performing the ALEPH/Dürr-Kambor analysis, one finds V/A breakdowns of $\sim 20 \pm 20\%\, V/80 \pm 20\%\, A$ for the w_{DK}- and $\hat{w}$-weighted IMFESR integral contributions from the combination of these two modes, the precise value varying by a few percent with variations in the choice of weight, the input effective 1400 width and fit window employed, and by $\sim 2\%$ over the range of s_0 considered in this analysis. While the reduction from $\pm 50\%$ to $\pm 20\%$, accomplished by taking into account the presence of the $K_1(1270)$ contributions, represents a significant improvement in the V/A separation uncertainty for the $K\pi\pi$ component of the us spectral integrals, one should bear in mind that the $K\pi\pi$ contribution is much smaller than the K and/or $K\pi$ ones, making the impact of this improvement on the errors in the total us spectral integrals much more modest.

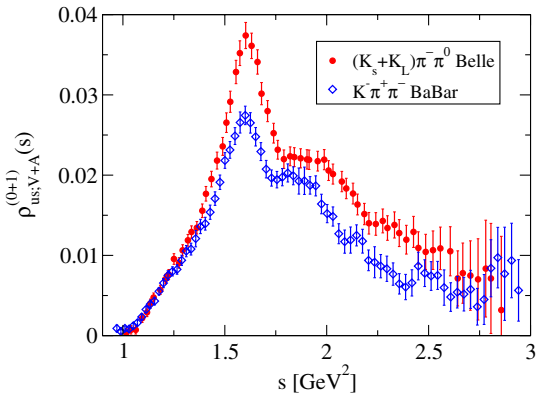

FIG. 2 (color online). The $K^-\pi^+\pi^-$ and $\bar{K}^0\pi^-\pi^0$ contributions to $\rho^{(0+1)}_{us;V+A}(s)$ implied by the *BABAR* $K^-\pi^+\pi^-$ [64] and Belle $\bar{K}^0\pi^-\pi^0$ [58] results presented at Tau 2012.

In the absence of high-statistics B-factory results for the distributions of the much smaller $K^-\pi^0\pi^0$ mode and all higher-multiplicity modes, we take the maximally conservative approach and assume a fully anticorrelated $50 \pm 50\%\, V/50 \pm 50\%\, A$ breakdown for the corresponding spectral integral contributions. Because of the anticorrelation, both for these modes, and in the separation of the 1400 region $K\pi\pi$ contributions, the total us spectral integral error is magnified for the $V - A$ difference. For the V, A and $V - A$ channels, where the V/A separation uncertainty plays a role, the suppression of contributions from the high-s region produced by the triple zeros of $w_{DK}(y)$ and $\hat{w}(y)$ at $s = s_0$ and the $1/s$ factor in the full weight $w(s)/s$ is especially important. The V/A separation uncertainty is, of course, absent for the V + A combination.

IV. RESULTS

The rhs's of the IMFESRs of Eqs. (8) and (9) are evaluated using the input specified in the previous section. Included in this input is the choice of the three-loop-truncated FOPT prescription for evaluating the $D = 2$ series. Since this choice was predicated on an agreement of the corresponding OPE representation and lattice data for Euclidean Q^2 extending from m_τ^2 down to, but not below, ~ 2 GeV^2, we restrict our attention to s_0 lying safely in this interval. With the ALEPH us data binning, this corresponds to 2.15 GeV$^2 \le s_0 \le m_\tau^2$. For s_0 in this range, experience with sum rules involving weights with a double zero at $s = s_0$ suggests integrated duality violations should also be negligible [34,35,66]. OPE contributions are very small for the $w_{DK}(y)$ version of the $\Delta\bar{\Pi}_{V-A}$ IMFESR, but less so for the $\hat{w}(y)$ version, where enhanced $D = 4$ contributions reach up to $\sim 8\%$ of the rhs in the s_0 window employed. OPE contributions are numerically relevant for both versions of the $\Delta\Pi_V$ and $\Delta\bar{\Pi}_{V+A}$ IMFESRs, reaching 6% and 8%, respectively, of the rhs's for the $w_{DK}(y)$ case, and 16% and 19%, respectively, of the rhs's for the $\hat{w}(y)$ case.

The dependences on s_0 of the OPE, continuum spectral integral and residual π/K-pole term contributions to the rhs's of the $w_{DK}(y)$ $\Delta\bar{\Pi}_{V+A}$ and $\Delta\bar{\Pi}_{V-A}$ IMFESRs, Eq. (9), are shown, for illustration, in Figs. 3 and 4. As noted already, OPE contributions are negligible for the latter, but not the former. Also shown are the totals of all three contributions, which should be independent of s_0 and equal to $\Delta\bar{\Pi}_{V+A}(0)$ and $\Delta\bar{\Pi}_{V-A}(0)$, respectively. The s_0 stability of these results is obviously excellent. Similarly good s_0 stability is found for the $w_{DK}(y)$ $\Delta\Pi_V$ IMFESR and all three $\hat{w}(y)$ IMFESRs. The corresponding figures are thus omitted for the sake of brevity. Given that OPE contributions to the $w_{DK}(y)$ $V - A$ IMFESR are numerically negligible, the stability of $\Delta\bar{\Pi}_{V-A}(0)$ with respect to s_0

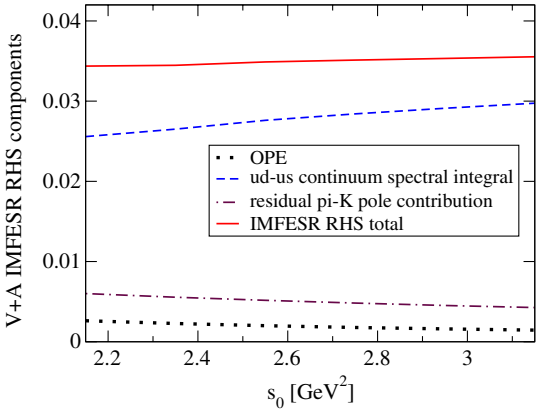

FIG. 3 (color online). Right-hand side contributions to the $w_{DK}(y)$ $\Delta\bar{\Pi}_{V+A}$ IMFESR, Eq. (9), as a function of s_0.

for this case supports the treatment of the exclusive *us* spectral integral contributions and V/A separation. The stability in the $V+A$ cases tests, in addition, the treatment of the OPE contributions. The s_0 stability in all cases also supports the neglect of higher-D OPE and residual duality-violating contributions in the analysis.

The values for $\Delta\Pi_V(0)$, $\Delta\bar{\Pi}_{V+A}(0)$ and $\Delta\bar{\Pi}_{V-A}(0)$ obtained from the $w_{DK}(y)$ analysis are as follows:

$$\begin{aligned}
\Delta\Pi_V(0) &= 0.0230(11)_{\rm cont}(4)_{OPE}(3)_{s_0} = 0.0230(12),\\
\Delta\bar{\Pi}_{V+A}(0) &= 0.0348(10)_{\rm cont}(2)_{\rm res}(5)_{OPE}(6)_{s_0} = 0.0348(13),\\
\Delta\bar{\Pi}_{V-A}(0) &= 0.0113(15)_{\rm cont}(2)_{\rm res}(3)_{OPE}(1)_{s_0} = 0.0113(15),
\end{aligned} \tag{22}$$

where, to be specific, the central values quoted represent the average over the s_0 window employed. The subscripts *OPE*, *cont* and *res* identify error components associated with OPE, continuum spectral integral and (where present) residual π/K-pole contributions, while the additional component labeled by the subscript s_0 specifies the small residual variation of the total over the s_0 analysis window.

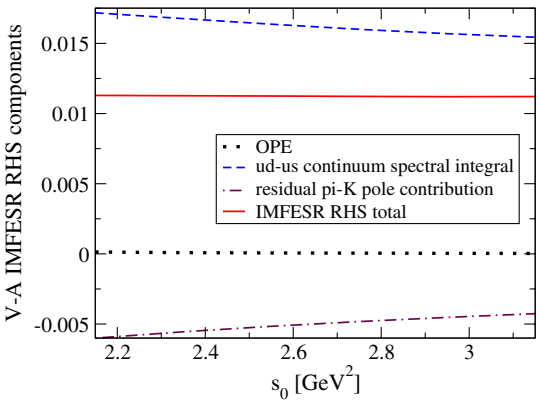

FIG. 4 (color online). Right-hand side contributions to the $w_{DK}(y)$ $\Delta\bar{\Pi}_{V-A}$ IMFESR, Eq. (9), as a function of s_0.

The $\hat{w}(y)$ versions of these analyses, similarly, yield

$$\begin{aligned}
\Delta\Pi_V(0) &= 0.0227(9)_{\rm cont}(6)_{OPE}(2)_{s_0} = 0.0227(10),\\
\Delta\bar{\Pi}_{V+A}(0) &= 0.0348(8)_{\rm cont}(2)_{\rm res}(8)_{OPE}(3)_{s_0} = 0.0348(12),\\
\Delta\bar{\Pi}_{V-A}(0) &= 0.0105(11)_{\rm cont}(2)_{\rm res}(5)_{OPE}(3)_{s_0} = 0.0105(13).
\end{aligned} \tag{23}$$

The agreement between the results of Eqs. (22) and (23) represents a further nontrivial test of the treatment of theoretical and spectral integral contributions. The total errors on $\Delta\Pi_V(0)$, $\Delta\bar{\Pi}_{V+A}(0)$ and $\Delta\bar{\Pi}_{V-A}(0)$ are rather similar for the $w_{DK}(y)$ and $\hat{w}(y)$ determinations, with spectral integral errors somewhat smaller and OPE errors somewhat larger for the $\hat{w}(y)$ case. In view of the similarity of the errors, and the fact that the $\hat{w}(y)$ analyses involve both significantly larger OPE contributions and integrated $D=2$ and $D=4$ OPE series having much slower convergence behavior, we take our final results to be those obtained from the $w_{DK}(y)$ IMFESRs, whose errors are dominantly experimental.

The results of Eq. (22), combined with the LEC contributions of Eq. (11), the LEC-independent contributions of Eq. (12), and the input values for $L^r_{5,9}(\mu_0)$, yield the final versions of the IMFESR constraints on the NNLO LEC combinations and (for $T=V$, $V-A$) L^r_{10}.

We now discuss in more detail the version of this analysis based on the weight w_{DK}. The $\hat{w}$-based analysis is analogous and, due to the good agreement between the results of Eqs. (22) and (23), leads to very similar results for the NNLO LECs. These will be displayed, together with those from the w_{DK} analysis, in Table II below.

The $w_{DK}(y)$ $T=V+A$ IMFESR becomes

$$\begin{aligned}
&C^r_{12}(\mu_0)+C^r_{61}(\mu_0)+C^r_{80}(\mu_0)\\
&\quad = 0.00248(13)_{\rm cont}(2)_{\rm res}(7)_{OPE}(9)_{s_0}(1)_{L^r_5}(8)_{L^r_9}\ {\rm GeV}^{-2}\\
&\quad = 0.00248(19)\ {\rm GeV}^{-2},
\end{aligned} \tag{24}$$

where the subscripts L^r_5 and L^r_9 label errors associated with the uncertainties on the input $L_{5,9}(\mu_0)$ values, and the labeling of all other sources of error is as specified above.

The $w_{DK}(y)$ $T=V-A$ IMFESR, similarly, yields

$$\begin{aligned}
&2.12L^r_{10}(\mu_0) - 32(m_K^2-m_\pi^2)[C^r_{12}(\mu_0)-C^r_{61}(\mu_0)+C^r_{80}(\mu_0)]\\
&\quad = -0.00346(145)_{\rm cont}(15)_{\rm res}(31)_{OPE}(8)_{s_0}(9)_{L^r_5}(61)_{L^r_9}\\
&\quad = -0.00346(161),
\end{aligned} \tag{25}$$

and the $w_{DK}(y)$ $T=V$ constraint

$$\begin{aligned}
&32(m_K^2-m_\pi^2)C^r_{61}(\mu_0)\\
&\quad = 0.00727(108)_{\rm cont}(38)_{OPE}(32)_{s_0}(9)_{L^r_5}(61)_{L^r_9}\\
&\qquad - 1.06L^r_{10}(\mu_0).
\end{aligned} \tag{26}$$

TABLE I. Previous results and estimates from the literature for $C^r_{12}(\mu_0)$, $C^r_{61}(\mu_0)$ and $C^r_{80}(\mu_0)$. LEC values are in units of GeV^{-2}.

LEC	RChPT		Quark model		Other
C^r_{12}	−0.00082	[26]	−0.00034(2)	[27]	0.00005(4) (Dispersive [67])
	−0.00044(16)	[68]			0.00057(10) (Lattice [12])
	−0.0008(4)	[69]			
C^r_{61}	0.0021	[17]	0.00288(26)	[27]	0.00081(38) (IMFESR [9])
	0.0019	[38]			
C^r_{80}	0.0021(5)	[69]	0.00087(4)	[27]	
	0.0019	[38]			

In Ref. [28], a combined fit incorporating the constraint, Eq. (25), the $\Pi_{ud;V-A}(0)$ constraint, Eq. (17), and lattice $\Pi_{ud;V-A}(Q^2)$ results for four $n_f = 2+1$, domain-wall fermion RBC/UKQCD ensembles (two with inverse lattice spacing $1/a = 2.31$ GeV and pion masses $m_\pi = 293$ and 349 MeV, and two with $1/a = 1.37$ GeV and $m_\pi = 171$ and 248 MeV), was shown to yield

$$L^r_{10}(\mu_0) = -0.00346(32), \tag{27}$$

$$\mathcal{C}^r_0(\mu_0) = -0.00034(13), \tag{28}$$

$$\mathcal{C}^r_1(\mu_0) = 0.0081(35). \tag{29}$$

The result in Eq. (28) corresponds to

$$C^r_{12}(\mu_0) - C^r_{61}(\mu_0) + C^r_{80}(\mu_0) = -0.00055(21)\ \text{GeV}^{-2}. \tag{30}$$

Equation (27), combined with the $T = V$ constraint, Eq. (26), then implies

$$\begin{aligned} C^r_{61}(\mu_0) &= 0.00151(15)_{\text{cont}}(5)_{OPE}(4)_{s_0}(1)_{L^r_5}(8)_{L^r_9}(5)_{L^r_{10}} \\ &\quad \times \text{GeV}^{-2} \\ &= 0.00151(19)\ \text{GeV}^{-2}. \end{aligned} \tag{31}$$

There is some correlation between the continuum spectral integral errors and L^r_{10}, but the impact of this correlation does not show up in the combined error, to the number of significant figures shown, since the error on L^r_{10} is strongly dominated by the errors on the lattice data.[6]

Taking into account the correlations between the V and $V+A$ analysis inputs (or, equivalently, performing the FB *ud-us A* IMFESR analysis directly), one finds, from Eqs. (24) and (31),

$$\begin{aligned} &C^r_{12}(\mu_0) + C^r_{80}(\mu_0) \\ &\quad = 0.00097(8)_{\text{cont}}(2)_{\text{res}}(4)_{OPE}(5)_{s_0}(5)_{L^r_{10}} \\ &\quad = 0.00097(11)\ \text{GeV}^{-2}. \end{aligned} \tag{32}$$

The determination of C^r_{12} in Ref. [10] has been recently updated to reflect new values for the main inputs $f_+(0)$ and f_K/f_π [67], with the result

$$C^r_{12}(\mu_0) = 0.00005(4)\ \text{GeV}^{-2}. \tag{33}$$

Equations (32) and (33) yield

$$C^r_{80}(\mu_0) = 0.00092(12)\ \text{GeV}^{-2}. \tag{34}$$

Replacing the inputs from Eq. (22) with those from Eq. (23) and repeating the steps just described yields the alternate $\hat{w}$ IMFESR determinations of the same NNLO LEC combinations shown in Table II. These are in excellent agreement with those obtained from the w_{DK} IMFESR analysis.

A number of estimates exist in the literature for the three NNLO LECs, $C^r_{12,61,80}(\mu_0)$, entering the combinations determined above. C^r_{61} was also obtained directly in an earlier version [9] of the FB V-channel IMFESR analysis,[7] and $C^r_{12}(\mu_0)$ (not determined here) in the lattice analysis of Ref. [12] and an updated version [67] of the coupled-channel dispersive analysis of Ref. [10]. These estimates/results are compiled in Table I. For the quark model results of Ref. [27], we quote, for simplicity, the larger of the two asymmetric errors from the original publication. In

[6]The impact of the uncertainties on L^r_5 and L^r_9 in the $T = V - A$ IMFESR constraint is also very small. As an example, doubling the L^r_9 uncertainty of Ref. [15] and rerunning the fit of Ref. [28], we find the errors in Eqs. (27), (28) and (29) shifted to 0.00033, 0.00015 and 0.0036, respectively, with no change in the central fitted values.

[7]A value for $C^r_{61}(\mu_0)$ differing from that in Table I was also given in Ref. [17]. This was meant to represent a translation of the Dürr-Kambor result [9], which was not given directly in terms of C^r_{61}, into the explicit C^r_{61} form. The two values turn out to differ because of a minor sign transcription error in the translation process. Thanks to Bachir Moussallam for clarifying the situation, and tracking down the source of the discrepancy.

TABLE II. Comparison of quark model and central RChPT estimates to the values of the NNLO LEC combinations obtained from the various IMFESR analyses above. LEC combinations are understood to be evaluated at $\mu = \mu_0$, and are in units of GeV^{-2}.

LEC combination	RChPT	Quark model	This work (w_{DK})	This work ($\hat{w}$)
$C^r_{12} + C^r_{61} + C^r_{80}$	0.0034	0.00341(27)	0.00248(19)	0.00248(18)
$C^r_{12} - C^r_{61} + C^r_{80}$	−0.0006	−0.00235(25)	−0.00055(21)	−0.00046(19)
C^r_{61}	0.0020	0.00288(26)	0.00151(19)	0.00147(17)
$C^r_{12} + C^r_{80}$	0.0014	0.00053(2)	0.00097(11)	0.00101(10)

Ref. [12], a number of different results were presented for C^r_{12}, corresponding to different fit strategies and inputs. Here only the result of fit IV, which did not employ data from the heavier $m_\pi = 556$ MeV ensemble and which used updated NLO LEC input (the preliminary version of the results of Ref. [26]), has been tabulated. Comparing the quark model and RChPT estimates to the IMFESR results above, one sees that the quark model does well for C^r_{80} but badly for C^r_{61}, while RChPT somewhat overestimates C^r_{61} and significantly overestimates C^r_{80}.

An alternate comparison, involving the combinations of NNLO LECs determined in the IMFESR analyses above, is given in Table II. Since errors are not quoted for some of the RChPT results in the literature, we present only central values in this case, using averages of the different RChPT results listed in Table I for each of the C^r_k's. It is worth noting that the result in Eq. (30) for $C^r_{12}(\mu_0) - C^r_{61}(\mu_0) + C^r_{80}(\mu_0)$ differs significantly from the value $0.00086(67)\ \text{GeV}^{-2}$ employed in Ref. [20]. The difference is due to a combination of two factors: a significant overestimate of C^r_{80} in the RChPT value used in Ref. [20], and the shift in the V-channel IMFESR result for C^r_{61} resulting from significant shifts in OPE and data inputs.

V. SUMMARY AND DISCUSSION

We have obtained rather good precision determinations of the NNLO LEC C^r_{61} and NNLO LEC combination $C^r_{12} + C^r_{61} + C^r_{80}$ through the use of FB IMFESRs. The much improved low-multiplicity B-factory strange hadronic decay distribution data plays an important role in achieving the reduced errors, as does the improved determination of L^r_{10} made possible by the lattice data on the flavor ud $V - A$ correlator. Our final results for the NNLO LECs are those given in the previous section.

The determinations based on w_{DK} and $\hat{w}$ are in excellent agreement, and both show good s_0 stability. Those based on w_{DK} have the additional advantage that the final errors are more dominated by their experimental components, and hence less dependent on the reliability of the estimates of OPE uncertainties, than are those based on $\hat{w}$. Because of the strong suppression of high-s spectral contributions for the weights employed, the us spectral integrals are dominated by contributions from the $K\pi$ mode, which has the most accurately measured of the strange exclusive distributions. For the $T = V + A$ case, where the us V/A separation uncertainties play no role, the result is that the errors on the ud continuum spectral integrals (which are a factor of ∼2 larger than the us continuum integrals) are slightly larger than the continuum us errors. Improvements to the errors on both the ud and us spectral distributions would thus be useful for further reducing the errors on our final results. For the $T = V$ and $V - A$ cases, in spite of the suppression of contributions from the higher-multiplicity modes, the us V/A separation uncertainty represents the largest component of the error on the us continuum spectral integrals.[8] The ud continuum errors, however, remain non-negligible, even for the $V - A$ case. For the w_{DK}-based IMFESRs, there is room for significant experimental improvement before reaching the limitations set by the OPE uncertainties. Improved V/A separation of the contributions from the $K\bar{K}\pi$ and $\bar{K}\pi\pi$ channels can, in principle, be made by angular analyses of the B-factory data for these modes, and such improvements would serve to significantly reduce the experimental components of the errors on the corresponding $T = V$ and $V - A$ IMFESR results.

With regard to the experimental errors, one should bear in mind that work on the strange distributions and branching fractions is ongoing. Preliminary *BABAR* results based on the Ph.D. thesis of Adametz [70], for example, show increases in the branching fractions of the $\tau^- \to K^- n\pi^0\nu_\tau$ modes. The dominant impact of such changes on the current analyses would be through the normalization of the $K^-\pi^0$-mode contributions, where the preliminary result $B[\tau^- \to K^-\pi^0\nu_\tau] = 0.00500(14)$ [70] differs significantly from the current PDG average 0.00429(15). ($\bar{K}^0\pi^-$ contributions, whose branching fraction normalization is a factor of about 2 larger, are, however, unaffected.) Rerunning the IMFESR analyses discussed above with the preliminary $B[\tau^- \to K^- n\pi^0\nu_\tau]$ results of Ref. [70] in place of those used previously and a concomitant adjustment to the global approximate ud V, A rescaling, one finds that $C^r_{12} + C^r_{61} + C^r_{80}$ and C^r_{61} are both shifted downwards by $\sim 1\sigma$, while C^r_{80} is left essentially unchanged. Explicitly, the results of the w_{DK} versions of these modified analyses are $C^r_{12}(\mu_0) + C^r_{61}(\mu_0) + C^r_{80}(\mu_0) =$

[8] As an example, at the midpoint, $s_0 = 2.65\ \text{GeV}^2$, of the s_0 analysis window, the ratio of the V/A separation uncertainty and $K\pi$ distribution error contributions to the error on the w_{DK}-weighted us spectral integral is ∼1.5 for the V channel and ∼3 for the $V - A$ channel.

$0.00230(18)\,\mathrm{GeV}^{-2}$, $C^r_{61}(\mu_0)$=0.00133(18)GeV^{-2}, and $C^r_{80}(\mu_0) = 0.00097(11)\mathrm{GeV}^{-2}$. We stress that *BABAR* has not yet released their final version of the analysis of the Adametz thesis data, so, at present, these results serve only to illustrate the potential impact of ongoing experimental work.

We also note that the RChPT estimates for the NNLO LECs considered here are not quantitatively reliable. This confirms the relevance of worries expressed elsewhere in the literature about some of the aspects of the RChPT approach [13,71,72].

Finally, we comment that the result of Ref. [28] for $\mathcal{C}^r_1(\mu_0)$, which corresponds to $C^r_{13}(\mu_0) - C^r_{62}(\mu_0) + C^r_{81}(\mu_0) = 0.00049(21)\,\mathrm{GeV}^{-2}$, provides another example of a $1/N_c$-suppressed LEC combination having a nonzero value for $N_c = 3$. Such combinations are usually neglected in making RChPT estimates, but the nonzero value in this case plays a nontrivial role in achieving the improved determination of L^r_{10} reported in Ref. [28]. We also note that the central value for this combination exceeds by a factor of ∼2.7 the bound

$$|C^r_{13}(\mu_0) - C^r_{62}(\mu_0) + C^r_{81}(\mu_0)| < |C^r_{12}(\mu_0) - C^r_{61}(\mu_0) + C^r_{80}(\mu_0)|/3 \qquad (35)$$

assumed for it in Ref. [20], where the $1/3$ on the rhs was meant to reflect the $1/N_c$ suppression of the lhs. This observation provides a cautionary note regarding the use of such large-N_c assumptions/bounds in contexts where they dominate the errors in the full analysis (in the case of Ref. [20], that on L^r_{10}).

ACKNOWLEDGMENTS

M. G. is supported in part by the U.S. Department of Energy. S. P. is supported by Grants No. CICYTFEDER-FPA2011-25948, No. SGR2009-894, and the Spanish Consolider-Ingenio 2010 Program CPAN (No. CSD2007-00042). K. M. is supported by a grant from the Natural Sciences and Engineering Research Council of Canada. K. M. would also like to thank Chen Shaomin, Denis Epifanov and Ian Nugent for providing details of the ALEPH, Belle and *BABAR* exclusive *us* spectral distributions, respectively.

APPENDIX: OPE CONTRIBUTIONS AND ERRORS

In this appendix, we provide details, broken down by dimension and source, of the total errors on the OPE contributions to the rhs's of the w_{DK} and $\hat{w}$ $T = V$, $V + A$ and $V - A$ IMFESRs quoted above. We remind the reader that the OPE terms in question represent contributions to the IMFESR determinations of the $Q^2 = 0$ values of the relevant FB correlator differences, and thus that the relevant scale for assessing the largeness or smallness of a given contribution is the corresponding $Q^2 = 0$ correlator value. To two significant figures these are, from either Eq. (22) or Eq. (23), $\Delta\Pi_V(0) = 0.023$, $\Delta\bar{\Pi}_{V+A}(0) = 0.035$ and $\Delta\bar{\Pi}_{V-A}(0) = 0.011$.

Table III lists our estimates of the central $D = 2$ contributions and errors, together with the individual contributions to these errors. The column headings δm^2, $O(\bar{a}^2)$, *Prescription* and $\delta\alpha_s$ label individual contributions associated with (i) the uncertainty on the overall squared mass factors arising from uncertainties in the FLAG quark mass inputs, (ii) a contribution to the truncation uncertainty equal to the size of the last $[O(\bar{a}^2)]$ term kept in the truncated series, (iii) the difference between the results for the three-loop-truncated series obtained using the central FOPT and alternate CIPT prescriptions, and (iv) the uncertainty induced by that on the $n_f = 5$ $\alpha_s(M_Z^2)$ input, respectively. We display results only for the smallest and largest s_0 employed, 2.15 and 3.15 GeV^2, respectively. All results decrease monotonically in magnitude with increasing s_0.

From the table, we see that $D = 2$ contributions are entirely negligible for $T = V - A$. The central $D = 2$ OPE contributions are also small, though not negligible, for the other channels, varying, for example for w_{DK}, from 5% to 3% of $\Delta\Pi_V(0)$ for $T = V$ and from 6% to 4% of $\Delta\bar{\Pi}_{V+A}(0)$

TABLE III. The w_{DK} and $\hat{w}$ IMFESR $D = 2$ OPE assessments, total errors and error components for the $T = V$, $V + A$ and $V - A$ channels and $s_0 = 2.15$ and 3.15 GeV^2. The s_0 entries are in GeV^2, and the error components are labeled as described in the text.

Weight	T	s_0	$D = 2$ integral	δm^2	$O(\bar{a}^2)$	*Prescription*	$\delta\alpha_s$
w_{DK}	V	2.15	0.00106(29)	0.00005	0.00011	0.00027	0.00002
		3.15	0.00061(13)	0.00003	0.00005	0.00012	0.00001
	$V + A$	2.15	0.00211(59)	0.00011	0.00022	0.00053	0.00003
		3.15	0.00121(26)	0.00006	0.00010	0.00023	0.00001
	$V - A$	2.15	−0.00001(1)	0.00000	0.00000	0.00000	0.00000
		3.15	−0.00000(0)	0.00000	0.00000	0.00000	0.00000
$\hat{w}$	V	2.15	0.00196(44)	0.00010	0.00038	0.00020	0.00004
		3.15	0.00109(20)	0.00006	0.00018	0.00007	0.00001
	$V + A$	2.15	0.00391(88)	0.00020	0.00075	0.00040	0.00007
		3.15	0.00219(40)	0.00011	0.00036	0.00015	0.00003
	$V - A$	2.15	0.00001(1)	0.00000	0.00001	0.00000	0.00000
		3.15	0.00001(0)	0.00000	0.00000	0.00000	0.00000

TABLE IV. The w_{DK} and $\hat{w}$ IMFESR $D = 4$ OPE estimates and total errors for the $T = V$, $V + A$ and $V - A$ channels and $s_0 =$ 2.15 and 3.15 GeV^2. The s_0 entries are in GeV^2.

Weight	T	s_0	$D = 4$ integral
w_{DK}	V	2.15	0.00028(7)
		3.15	0.00013(3)
	$V + A$	2.15	0.00051(15)
		3.15	0.00024(7)
	$V - A$	2.15	0.00006(2)
		3.15	0.00002(1)
$\hat{w}$	V	2.15	0.00173(39)
		3.15	0.00080(18)
	$V + A$	2.15	0.00270(76)
		3.15	0.00129(36)
	$V - A$	2.15	0.00077(32)
		3.15	0.00030(12)

for $T = V + A$, as s_0 is increased from 2.15 to 3.15 GeV^2. The corresponding total $D = 2$ errors, similarly, vary from 1% to 0.6% of $\Delta\Pi_V(0)$ and from 2% to 0.7% of $\Delta\bar{\Pi}_{V+A}(0)$ over the same range. The prescription dependence is the dominant contribution to the total error for w_{DK}, while both the prescription dependence and $O(\bar{a}^2)$ truncation error contribution play a significant role for $\hat{w}$. The $D = 2$ errors for $\hat{w}$ are ~50% larger than those for w_{DK}.

Table IV contains our $D = 4$ contributions and total errors. The errors are the quadrature sum of (i) the uncertainty generated by that on the input FLAG ratio of strange to light quark masses, (ii) a truncation uncertainty equal to the last $[O(\bar{a}^2)]$ term kept in the truncated $D = 4$ series, and (iii) the uncertainty generated by that on r_c. Since the r_c-induced uncertainty is much larger than the other two, we quote only the total error in this case. $D = 4$ errors for the V and $V + A$ channels are much smaller than the corresponding $D = 2$ errors for w_{DK}, but grow to ~90% of the corresponding $D = 2$ errors for $\hat{w}$. The $D = 4$ contributions are also subleading (~20%–25% of the $D = 2$ ones) in the V and $V + A$ channels for w_{DK}. For $\hat{w}$, in contrast, they range from 88% to 73% and from 69% to 58% of the $D = 2$ contributions for the V and $V + A$ channels, respectively. $D = 4$ $V - A$ contributions, though larger than the strongly suppressed $D = 2$ ones, are still very small for w_{DK} and do not exceed 7% of $\Delta\bar{\Pi}_{V-A}(0)$ for $\hat{w}$.

As noted in the text, a very conservative error, equal to the value of the *ud* contribution to the FB difference, is employed for the sum of the FB $D = 6$ and 8 contributions.

TABLE V. $s_0 = 2.15$ and 3.15 GeV^2 values of the estimated FB $D = 6 + 8$ contributions, together with the flavor *ud* $D = 6 + 8$ OPE contributions and errors used to set the uncertainty on the estimated central values, for the $T = V$, $V + A$ and $V - A$ channel versions of the w_{DK} and $\hat{w}$ IMFESRs. The s_0 entries are in GeV^2.

Weight	T	s_0	Central *ud-us* $D = 6 + 8$ integral	*ud* $D = 6 + 8$ integral
w_{DK}	V	2.15	−0.00000	0.00048(20)
		3.15	−0.00000	0.00013(5)
	$V + A$	2.15	0.00000	0.00011(47)
		3.15	0.00000	0.00002(13)
	$V - A$	2.15	−0.00001	0.00045(17)
		3.15	−0.00000	0.00013(4)
$\hat{w}$	V	2.15	0.00001	−0.00053(22)
		3.15	0.00000	−0.00017(7)
	$V + A$	2.15	−0.00001	0.00001(51)
		3.15	−0.00000	0.00000(16)
	$V - A$	2.15	0.00002	−0.00066(11)
		3.15	0.00001	−0.00021(4)

The central value is obtained using the VSA for the $D = 6$ contributions and setting $D = 8$ contributions to zero. The *ud* contribution used to set the error on this (very small) central value is evaluated for $T = V$ and $V + A$ using the fit values for C_6^V, C_6^A, C_8^V and C_8^A obtained in Ref. [35], and for $T = V - A$ using the direct fits for the $V - A$ channel analogues, C_6^{V-A} and C_8^{V-A}, obtained in Ref. [21]. The resulting central *ud-us* $D = 6 + 8$ estimates, together with the *ud* $D = 6 + 8$ contributions and their errors (the latter generated by the errors and correlations on the fitted $D = 6$ and 8 coefficients) are listed in Table V. For $T = V + A$, there are strong cancellations between the separate V and A contributions, with the result that the central value of the $D = 6 + 8$ *ud* $V + A$ sum is much smaller than the corresponding uncertainty. No such strong cancellation occurs in either of the V or $V - A$ channels. To maintain our $D = 6 + 8$ bound as a conservative one for all three cases, we have thus taken as the final versions of the error bounds on the FB *ud-us* $D = 6 + 8$ contributions the sum of the absolute values of the corresponding central *ud* contribution and its error. These can be read off directly from the results quoted in the table. The resulting $D = 6 + 8$ error is the largest of the OPE error components for the V and $V - A$ channels, and non-negligible, but somewhat smaller than the $D = 2$ error, for $V + A$.

[1] S. Weinberg, Physica (Amsterdam) **96A**, 327 (1979).
[2] J. Gasser and H. Leutwyler, Ann. Phys. (N.Y.) **158**, 142 (1984).
[3] J. Gasser and H. Leutwyler, Nucl. Phys. **B250**, 465 (1985).
[4] H. W. Fearing and S. Scherer, Phys. Rev. D **53**, 315 (1996).

[5] J. Bijnens, G. Colangelo, and G. Ecker, J. High Energy Phys. 02 (1999) 020; Ann. Phys. (N.Y.) **280**, 100 (2000).
[6] M. Knecht, B. Moussallam, and J. Stern, Nucl. Phys. **B429**, 125 (1994).
[7] E. Golowich and J. Kambor, Phys. Rev. D **53**, 2651 (1996).
[8] K. Maltman, Phys. Rev. D **53**, 2573 (1996); K. Maltman and C. E. Wolfe, Phys. Rev. D **59**, 096003 (1999).
[9] S. Dürr and J. Kambor, Phys. Rev. D **61**, 114025 (2000).
[10] M. Jamin, J. A. Oller, and A. Pich, J. High Energy Phys. 02 (2004) 047.
[11] V. Bernard and E. Passemar, Phys. Lett. B **661**, 95 (2008).
[12] V. Bernard and E. Passemar, J. High Energy Phys. 04 (2010) 001.
[13] G. Ecker, P. Masjuan, and H. Neufeld, Phys. Lett. B **692**, 184 (2010).
[14] G. Ecker, P. Masjuan, and H. Neufeld, Phys. Lett. B **692**, 184 (2010).
[15] J. Bijnens and P. Talavera, J. High Energy Phys. 03 (2002) 046.
[16] J. Bijnens and P. Dhonte, J. High Energy Phys. 10 (2003) 061.
[17] K. Kampf and B. Moussallam, Eur. Phys. J. C **47**, 723 (2006).
[18] P. Büttiker, S. Descotes-Genon, and B. Moussallam, Eur. Phys. J. C **33**, 409 (2004).
[19] G. Colangelo, J. Gasser, and H. Leutwyler, Nucl. Phys. **B603**, 125 (2001).
[20] M. González-Alonso, A. Pich, and J. Prades, Phys. Rev. D **78**, 116012 (2008).
[21] D. Boito, M. Golterman, M. Jamin, K. Maltman, and S. Peris, Phys. Rev. D **87**, 094008 (2013).
[22] G. Ecker, J. Gasser, A. Pich, and E. de Rafael, Nucl. Phys. **B321**, 311 (1989).
[23] See, e.g., A. Pich, *Proc. Sci.*, Confinement8 (**2008**) 026, and references cited therein.
[24] See, e.g., M. Knecht and A. Nyffeler, Eur. Phys. J. C **21**, 659 (2001); V. Cirigliano, G. Ecker, M. Eidemüller, R. Kaiser, A. Pich, and J. Portolés, Nucl. Phys. **B753**, 139 (2006); I. Rosell, J. J. Sanz-Cillero, and A. Pich, J. High Energy Phys. 01 (2007) 039; A. Pich, I. Rosell, and J. J. Sanz-Cillero, J. High Energy Phys. 07 (2008) 014; 02 (2011) 109.
[25] J. Gasser, C. Haefeli, M. A. Ivanov, and M. Schmid, Phys. Lett. B **652**, 21 (2007).
[26] J. Bijnens and I. Jemos, Nucl. Phys. **B854**, 631 (2012).
[27] S. Z. Jiang, Y. Zhang, C. Li, and Q. Wang, Phys. Rev. D **81**, 014001 (2010).
[28] P. A. Boyle *et al.* (unpublished); see also P. A. Boyle *et al.*, *Proc. Sci.*, LATTICE2012 (**2012**) 156, and the link to the slides of the Lattice 2013 talk by K. Maltman, www.lattice2013.uni-mainz.de/static/SMR.html#contrib3842.
[29] Y.-S. Tsai, Phys. Rev. D **4**, 2821 (1971).
[30] J. Erler, Rev. Mex. Fis. **50**, 200 (2004).
[31] M. Jamin, J. A. Oller, and A. Pich, Nucl. Phys. **B587**, 331 (2000); **B622**, 279 (2002); Phys. Rev. D **74**, 074009 (2006).
[32] K. Maltman and J. Kambor, Phys. Rev. D **65**, 074013 (2002).
[33] K. Maltman, Phys. Lett. B **440**, 367 (1998); C. A. Dominguez and K. Schilcher, Phys. Lett. B **448**, 93 (1999).
[34] D. Boito, O. Catà, M. Golterman, M. Jamin, K. Maltman, J. Osborne, and S. Peris, Phys. Rev. D **84**, 113006 (2011).
[35] D. Boito, M. Golterman, M. Jamin, A. Mahdavi, K. Maltman, J. Osborne and S. Peris, Phys. Rev. D **85**, 093015 (2012).
[36] K. Maltman, Phys. Rev. D **58**, 093015 (1998).
[37] K. Maltman and J. Kambor, Phys. Rev. D **64**, 093014 (2001).
[38] G. Amoros, J. Bijnens, and P. Talavera, Nucl. Phys. **B568**, 319 (2000).
[39] J. Beringer *et al.*, Phys. Rev. D **86**, 010001 (2012).
[40] See G. Colangelo *et al.*, Eur. Phys. J. C **71**, 1695 (2011); A. Jüttner *et al.*, arXiv:1109.1388; and updates accessible from the main page of the 2013 FLAG compilation, which may be found at itpwiki.unibe.ch/flag/index.php/Review_of_lattice_result_concerning_low_energy_particle_physics.
[41] M. Davier, L. Girlanda, A. Höcker, and J. Stern, Phys. Rev. D **58**, 096014 (1998).
[42] E. Shintani, S. Aoki, H. Fukaya, S. Hashimoto, T. Kaneko, H. Matsufuru, T. Onogi, and N. Yamada, Phys. Rev. Lett. **101**, 202004 (2008).
[43] P. A. Boyle, L. Del Debbio, J. Wennekers, and J. M. Zanotti, Phys. Rev. D **81**, 014504 (2010).
[44] K. Ackerstaff *et al.* (OPAL Collaboration), Eur. Phys. J. C **7**, 571 (1999).
[45] R. Barate *et al.* (ALEPH Collaboration), Z. Phys. C **76**, 15 (1997); R. Barate *et al.* (ALEPH Collaboration), Eur. Phys. J. C **4**, 409 (1998); S. Schael *et al.* (ALEPH Collaboration), Phys. Rep. **421**, 191 (2005).
[46] D. R. Boito, O. Catà, M. Golterman, M. Jamin, K. Maltman, J. Osborne, and S. Peris, Nucl. Phys. B, Proc. Suppl. **218**, 104 (2011).
[47] C. Aubin and T. Blum, Phys. Rev. D **75**, 114502 (2007).
[48] K. G. Chetyrkin and A. Kwiatkowski, Z. Phys. C **59**, 525 (1993).
[49] P. A. Baikov, K. G. Chetyrkin, and J. H. Kuhn, Phys. Rev. Lett. **95**, 012002 (2005).
[50] D. J. Broadhurst and S. C. Generalis, Open University Report No. OUT-4102-12, 1984; S. C. Generalis, J. Phys. G **15**, L225 (1989); K. G. Chetyrkin, S. G. Gorishnii, and V. P. Spiridonov, Phys. Lett. B **160**, 149 (1985).
[51] E. Braaten, S. Narison, and A. Pich, Nucl. Phys. **B373**, 581 (1992).
[52] T. van Ritbergen, J. A. M. Vermaseren, and S. A. Larin, Phys. Lett. B **400**, 379 (1997); K. G. Chetyrkin, Phys. Lett. B **404**, 161 (1997); T. Van Ritbergen, J. A. M. Vermaseren, and S. A. Larin, Phys. Lett. B **405**, 327 (1997); M. Czakon, Nucl. Phys. **B710**, 485 (2005).
[53] K. G. Chetyrkin, B. A. Kniehl, and M. Steinhauser, Phys. Rev. Lett. **79**, 2184 (1997).
[54] C. McNeile, A. Bazavov, C. Davies, R. Dowdall, K. Hornbostel, G. Lepage and H. Trottier, Phys. Rev. D **87**, 034503 (2013).
[55] M. Jamin and B. O. Lange, Phys. Rev. D **65**, 056005 (2002).
[56] See, e.g., K. Maltman, Nucl. Phys. B, Proc. Suppl. **218**, 146 (2011) and references cited therein.
[57] See P. A. Boyle *et al.*, *Proc. Sci.*, ConfinementX (**2012**) 100 and the link to the slides of the talk by K. Maltman at PhiPsi13, agenda.infn.it/contributionDisplay.py?sessionId=26&contribId=10&confId=5428.
[58] S. Ryu (Belle Collaboration), arXiv:1302.4565.

[59] J. H. Kühn and E. Mirkes, Z. Phys. C **56**, 661 (1992); **67**, 364(E) (1995).
[60] R. Barate *et al.*, Eur. Phys. J. C **11**, 599 (1999). Thanks to Shaomin Chen for providing the details of the exclusive mode contributions to the inclusive distribution.
[61] B. Aubert *et al.* (*BABAR* Collaboration), Phys. Rev. D **76**, 051104 (2007).
[62] D. Epifanov *et al.* (Belle Collaboration), Phys. Lett. B **654**, 65 (2007). Thanks to Denis Epifanov for providing access to the $K_s\pi^-$ invariant mass spectrum, which may be found at belle.kek.jp/belle/preprint/2007-28/tau_kspinu.dat.
[63] I. M. Nugent, Ph.D. thesis, University of Victoria, 2009.
[64] I. M. Nugent, arXiv:1301.7105. Thanks to Ian Nugent for providing the unfolded $K^-\pi^-\pi^+$ distribution and covariances presented in this paper.
[65] J. C. Hardy and I. S. Towner, Phys. Rev. C **79**, 044402 (2009).
[66] K. Maltman and T. Yavin, Phys. Rev. D **78**, 094020 (2008).
[67] M. Jamin (private communication). The new result reflects updated FLAG values for the inputs $f_0(0)$ and f_K/f_π of the original analysis.
[68] V. Cirigliano, G. Ecker, M. Eidemüller, R. Kaiser, A. Pich and J. Portolés, J. High Energy Phys. 04 (2005) 006.
[69] R. Unterdorfer and H. Pichl, Eur. Phys. J. C **55**, 273 (2008).
[70] A. Adametz, Ph.D. thesis, University of Heidelberg, 2011; *BABAR* Collaboration (to be published).
[71] M. Golterman and S. Peris, Phys. Rev. D **74**, 096002 (2006).
[72] P. Masjuan and S. Peris, J. High Energy Phys. 05 (2007) 040.